Novel fluid dynamic nonlinear numerical models of servovalves for aerospace

Novel fluid dynamic nonlinear numerical models of servovalves for aerospace

Matteo D. L. Dalla Vedova, and Parid Alimhillaj

***Abstract*— Modern** flight control system often requires the development of more and more highly detailed numerical simulation models in order to analyze their specific behavior as a whole or related to their components and subsystems. Especially during preliminary design activities or in the development of diagnostic or prognostic algorithms, it is often required to implement simplified numerical models able to simulate the actual behavior of the considered system, combining appropriate levels of accuracy and reliability with low calculation times and moderate computational efforts. In this work, authors investigated the feasibility of new simplified numerical models, aiming to provide faster models able to analyze the dynamic behavior of entire systems and, at the same time, able to guarantee a suitable level of accuracy. In particular, this paper concerns novel fluid-dynamics numerical models simulating the performance of servovalves. These algorithms are based upon a semi-empirical formulation and, although simplified, they are able to take calculate the effects of variable supply pressure and leakages (which is related to the control ports connecting the valve to the motor elements). Two new models are proposed and compared with a detailed reference. This comparison is performed by evaluating the performance of the different models and their ability to describe the fluid dynamic behavior of the considered valve.

***Keywords*—** Fluid-dynamic, Hydraulic, Servovalve, Simulation, Simplified numerical model.

I. Introduction

IN today's civil and military airplanes, the complexity of flight control systems is progressively increasing, but based on the very strict standards typical of the aeronautics industry, these control systems must also meet stringent requirements regarding their performance and in particular their safety. Therefore, the design and design of these systems today provides for the use of highly detailed numerical models, capable of predicting or analyzing their behavior with sufficient accuracy (at the system level as well as the subsystem or component level). The implementation of more simplified and fast models is beneficial in terms of control systems efficacy (i.e. enhancing their performances in online dynamic simulation), but it is necessary to guarantee suitable performances in all considered systems working conditions (and, in particular, in case of high workload regimes associated with real-time computerized analysis of systems monitoring tasks). Therefore, especially in the preliminary design or development phases of diagnostic or prognostic algorithms in real time (or almost in real time), it is essential to prepare simplified numerical models capable of combining sufficient levels of accuracy and reliability with reduced CPU calculation times and/or computational costs. These simplified numerical models (SNM) are particularly suitable for monitoring systems, both on the ground and in flight; in fact, since these functions must be performed in real time, they can require a high computational load for the on-board processors of the aircraft and therefore the implementation of lighter algorithms can be advantageous. From an operational point of view, these numerical models can be applied to the basic components of any proportional hydraulic control system, i.e. hydraulic control-valves, servovalves (SVs), electrohydraulic or hydromechanical actuators, etc.

M. D. L. Dalla Vedova is with the Department of Mechanical and Aerospace Engineering (DIMEAS), Politecnico di Torino, Corso Duca degli Abruzzi, 24 - 10129 - Torino, ITALY. (corresponding author phone: +390110906850; e-mail: matteo.dallavedova@polito.it).

P. Alimhillaj is with the Department of Energy, Faculty of Mechanical Engineering, Polytechnic University of Tirana, Mother Teresa Square, 4 - 1001 - Tirana, ALBANIA. (e-mail: palimhillaj@albcontrol.al).

II. Considered Numerical Test Bench

In this paper authors refer to a four-ways type control valve (named respectively supply port S, return port R, control port 1, control port 2) shown in Fig. 1, coupled with a linear jack through the two control ports (Fig. 2). The valve spool displacement XS controls the opening/closing of the four passageways, characterized by their overlaps/underlaps and connecting each control port to the supply and return ports respectively, so providing the desired relationship between flow and absolute pressure concerning each control port (named P1 and P2), under defined oil characteristics [1-2]. The corresponding differential pressure, regulated between the two control ports is named P12. In zero-flow conditions, each control port absolute pressure is close to the supply one when the related passageway is much more open than the return one, and particularly for spool displacements performing a return passageway fully closed (saturation condition) [3-5].

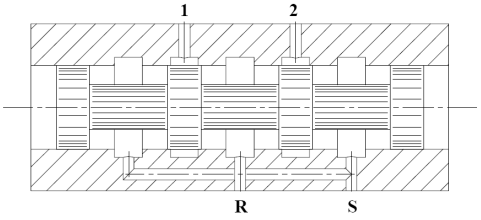

Fig. 1 schematic of the considered four ways valve

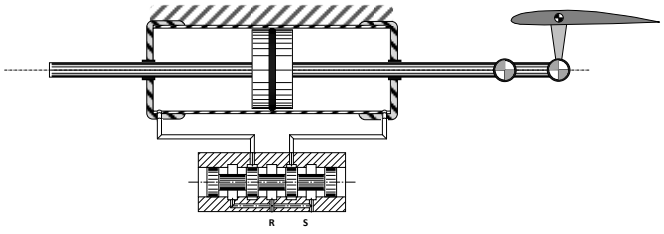

Fig. 2 schematic of the considered onboard hydraulic actuator

In the opposite case, the control port absolute pressure is close to the return one; in intermediate conditions, the control port pressures acquire medium amounts, having a progressive evolution between return pressure (PR) and supply pressure (PS) values, as it can be seen in the fluid-dynamic valve characteristic P12-XS plotted in Fig. 3.

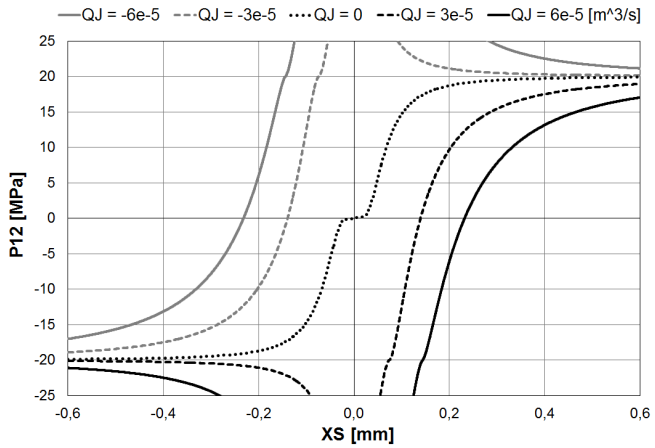

Fig. 3 valve characteristic P12-XS (HD fluid dynamic model)

It must be noted that the said valve characteristic P12-XS is a graph representing the evolution of the differential pressure P12 regulated by the valve as a function of the spool displacement XS and parameterized in the flow QJ provided to the user for a given valve geometry). In case of non-zero flow conditions, the obtained differential control ports pressures P12 may be markedly different with respect to zero flow conditions, particularly in case of small spool displacement; this behavior is related to pressure losses due to the oil flow QJ which is forced to flow through the valve regulating doors. Figure 3 has been simulated by means of a detailed lumped numerical model (named HD fluid dynamic model) formerly proposed by Jacazio et al. in [3-4] and enhanced by Borello et al. [5]. The accuracy of this model has been verified by comparing its outputs with the experimental results obtained by Urata [6-12] (as regards the servovalve electromechanical modelling), whereas the valve fluid dynamic model has been validated by certified numerical codes (e.g. Amesim or CFD softwares) and experimental data [13-17].

III. Simplified SV Fluid Dynamic Models

Several model describing the fluid-dynamic behaviors of valves are available in the literature, but must be noted that only detailed high-fidelity approaches, not explicitly dealt with in this work, are generally proper to describe the behavior shown in Fig. 3, evaluating the interactions between flow and absolute pressure regulated across each control port [14]; when simpler and quicker models are requested or desired, as in the present work, only the controlled differential pressure between the two control ports P12 and a single flow value QJ (common to both control ports) are usually computed.

A. Simplified Fluid Dynamic Models in Literature

Basically exist two main categories of fluid-dynamic control valve numerical models: a first type, suitable for regulating the controlled differential pressure acting on the motor element (e.g. linear actuators or hydraulic motors) and the other controlling the regulated flow in output [18]. As reported in [19], the former type describes the relationship between an output variable (i.e. the differential pressure imposed on the motor element) and an input variable (i.e. the commanded valve spool displacement), having as the feedback action the controlled flow through the motor element itself. As these categories of models have a multi-purpose generalist nature the aforesaid considerations are mostly valid in several cases, as the detailed complex model and the simplified ones considered in this work. The second category of fluid dynamic models that will be not considered in this paper gives the controlled flow as the output variable and uses the differential pressure as a feedback input, while the spool displacement is still assumed as the control input. In general, as regards the valve simplified numerical models available in the literature, the fluid-dynamic behavior is often simulated through a linearized approach based on two coefficients, easily obtainable experimentally, defined respectively pressure gain (GP) and flow gain (GQ) [20]. Therefore, adopting the said linear approach, it is possible to conceive the most simplified numerical model shown in Fig. 4: the spool displacement XS, through the valve pressure gain GP, produces a proportional value of differential pressure P12, which act on the motor element; this pressure is reduced by the pressure losses which are related to the controlled flow passing through the pressure/flow gain ratio GPQ. The most important weakness of this modeling is constituted to its impossibility to accurately simulate the effects of the supply pressure limits and, consequently, to calculate the actual stall conditions of the motor element.

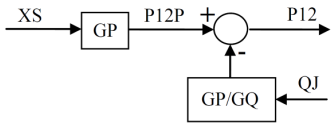

Fig. 4 linearized numerical model of the valve fluid dynamics

It must be noted that this linearized numerical model (shown in Fig. 4) is not able to take into account the effects due to the maximum value of differential pressure PSR provided by the hydraulic supply or to an eventual pressure supply drops (e.g. a partial depressurization of the hydraulic system).

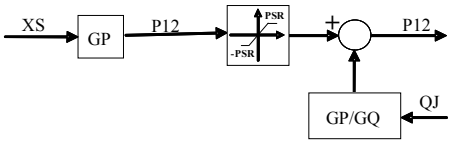

Fig. 5 nonlinear numerical model of the valve fluid dynamics

To this purpose, a possible variant (derived from the previously described model) is reported in Fig. 5: it consists of the implementation of a saturation block acting on the differential pressure developed through the related gain. In this way, it is possible to progressively enhance the model performance computing the effects of the differential supply pressure PSR. It must be noted that the so described model has a severe shortcoming, underestimating the actuation rate in case of a fully open valve: this is particularly noticeable when the valve reaches the saturation condition for small spool strokes (if compared with its maximum displacement XSM).

In a previous work [19], the authors proposed four new simplified numerical models (A, B and C-type briefly shown in the next section) derived to the ones described here above: they have been conceived to better simulate the differential pressure limits which are connected to the hydraulic power supply. However, all these models highlight, even if to a different extent, the same limits, essentially relate to their ability to correctly evaluate the effects of leakages and variable supply pressure (PS). Moreover, as regards the C-type models, the numerical simulation of these leakages produces an instantaneous computational feedback loop that can generate numerical instabilities and convergence problems.

B. Simplified fluid dynamic models A, B, C1 and C2

The approach proposed by the authors in [19] takes into account the effects of the variable values of the supply/return differential pressure performed by the hydraulic system, (reported as PSR): to this purpose, it must be noted that the effect of PSR on both pressure (GP) and flow (GQ) gain amounts can be computed in a reasonable but simple form by considering the general layout of the models, which is as linear as possible and, consequently, is conceived around the acceptable hypothesis of a linear relationship between each considered gain and the value of PSR. The actual values of GP are sufficiently close to the proportionality with respect to PSR, but the actual values of GQ are more and more close to the proportional to the square root of PSR. In this situation, it can be assumed that the proportionality between the GQ and the PSR it is not so realistic, but it will be accepted in our models as it is in line with the proposed linearized approach. Therefore, the pressure to flow gain ratio (GP/GQ) can be assumed as independent on the value of PSR. In the same way, also the value of the spool displacement XS at which the differential pressure P12, produced on the motor element in the zero-flow condition (defined P12P), saturates to PSR can be considered independent on PSR; this critical spool displacement (hereafter reported as XSS) is characteristic of the different types of valves and dependent on the internal geometry of the spool. According to these assumptions, the value of P12P can be computed dividing XS by XSS and multiplying it by the value assumed by PSR in the present situation, as shown in Fig. 9; further, the pressure to flow gain ratio GP/GQ can be replaced by the coefficient GPQ, which is invariant with respect to the supply differential pressure PSR.

As regards the leakage model and related computational algorithm, the authors introduced the following considerations. The aforesaid leakage is modeled as the sum of all the fluid-dynamic losses that determine oil flows through the sealing elements of the valve spool. In other words, the flow controlled by the valve passageways, and driven to the ports 1 and 2 (Fig. 1), mainly operates across and within the motor element, displacing a proper fluid volume and developing mechanical power, but, usually, a small amount of it flows, across imperfect seals or intentional bypass devices (based on calibrates orifices), directly from port 1 to 2 or vice versa (so being unable to perform any useful work). Nevertheless, it produces further pressure losses across the valve passageways, besides those developed by the operating flow. Also in this case it is reasonable to assume a linear dependence between the differential pressure P12 and the leakage flow drained (QLk); this simplified hypothesis is generally admissible as it is assumed that leakage generates small oil amounts flowing through very small dimension passages. So, the relationship between P12 and QLk should be expressed as follows:

$$QLk = CLk \cdot P12 \tag{1}$$

where the CLk is the leakage coefficient. As depicted in Fig. 6, the valve leakage can be modeled by the feedback loop containing the CLk block; it must be noted that CLk represents the ratio between the leakage flow QLk and the differential pressure P12 (which generates this fluid loss).

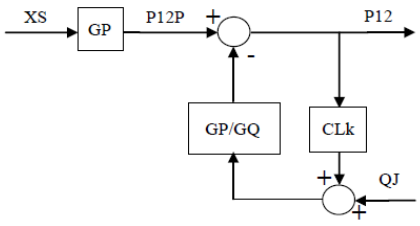

Fig. 6 linear fluid dynamic model sensitive to valve leakage

The total oil flow disposing through the valve control passageways should be calculated summing the leakage flow QLk and the controlled working flow QJ; also it can obtain the related differential pressure loss multiplying it by the pressure/flow gain ratio GPQ. It must be noted that the computational structure shown in Fig. 7 is afflicted to a meaningful numerical shortcoming: the leakage feedback branch, containing only algebraic blocks, constitutes an instantaneous loop causing numerical instabilities. This problem is overcome rewriting the computational algorithm by

a different formulation based on the preventive analytical solution of the said leakage instantaneous loop (Fig. 8). Starting from the block diagram shown in Fig. 8, authors proposed in [19] a development of the said linear fluid dynamic model (Fig. 6), which takes into account the effects of leakage and variable supply differential pressure PSR: this model, named MODEL A, is shown in Fig. 9. Taking into consideration the same effects of the variable value of PSR as well the leakage, it is possible to develop the nonlinear model represented in Fig. 2, obtaining another configuration, named MODEL B (Fig. 10). However, as reported in [19], this modeling, although more complex than the previous one, is completely unsatisfactory.

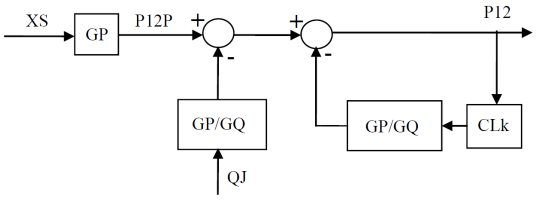

Fig. 7 reformulation of Fig. 6 by separating QJ and CLk loops

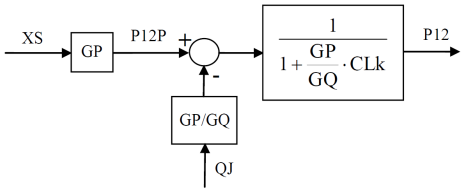

Fig. 8 valve leakage loop solution

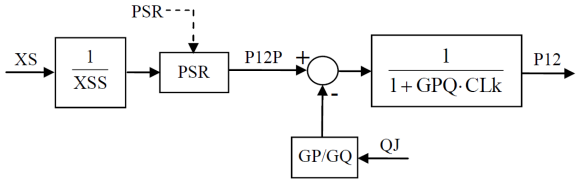

Fig. 9 MODEL A: linear valve model sensitive to PSR and CLk [19]

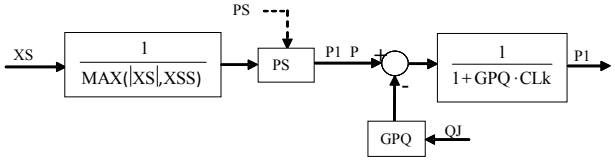

Fig. 10 MODEL B: non-linear valve model sensitive to PSR and CLk

A modified version of the nonlinear numerical model shown in Fig. 5 have been proposed in [20]; the main difference regards the position of the pressure saturation block which, in this alternative case, is positioned downstream the flow feedback, as it can be seen in Fig. 11.

The advantage offered by this layout consists of the ability to take acceptably into account the effects of P12 limitations on the actuation rate, so obtaining a more proper value of the no-load actuation rate itself. On the contrary, the shortcoming of this model is represented by the inability to simulate the temporary overload conditions, eventually affecting the motor element. In this layout, the weak evaluation of overload conditions is generally not considered so important, and, vice-versa, the better performance in evaluating the motor actuation speed (providing in this way a more precise value of the no-load actuation rate) is significantly considered. Several models/algorithms has been developed starting from the block diagram of Fig. 11 to analyze the fluid dynamic behavior of a given valve taking into account the effects due to leakage and differential supply pressure PSR [19-20]. The main goal of these nonlinear models was combining two opposite, and often antithetical, characteristics: the maximum simplicity to represent the physical system (i.e. reduced computational burdens) and the required high accuracy (i.e. its fidelity in simulating the actual fluid dynamic behavior).

A first model derived from the scheme of Fig. 11, named MODEL C1 in [19], is shown in Fig. 12. It includes leakage and variable PSR computational algorithms and the flow feedback sum block, nevertheless being upstream the saturation block PSR, has been displaced downstream the GP one in order to use the invariant GPQ block. In this way, the leakage feedback loop is fully located downstream the pressure saturation block, limited within the values ± PSR.

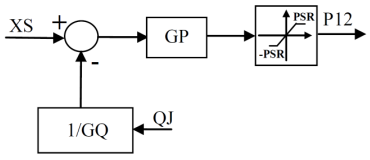

Fig. 11 Alternative nonlinear model of the valve fluid dynamics

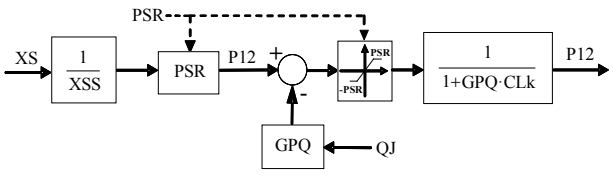

Fig. 12 Fig. MODEL C1 block diagram [19]

MODEL C1 must be able to simulate the effect of variable values of PSR along the simulation run, evaluating (according to the above-discussed assumption of proportionality between GP, GQ and PSR) the relative variable values of pressure and flow gains. Furthermore, the leakage feedback loop must be previously analytically solved, to avoid problems of computational instability. Another model derived from the scheme shown in Fig. 11, that has been defined as MODEL C2 in [19], is depicted in Fig.13.

In this formulation the leakage loop is entirely located upstream the pressure saturation block, limited within the values ± PSR. As widely described by the authors in [19], the major drawback of both MODEL C1 and C2 is related to the pressure gain contained in GPQ coefficient that, not taking into account the differential pressure saturation, could generate shortcomings regarding the evaluation of the leakage effects.

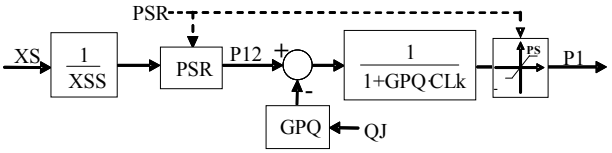

Fig. 13 MODEL C2 block diagram [19]

IV. Proposed Simplified Fluid Dynamic Model

In this paper, the authors will propose some new synthetic formulations which are intended to enhance the behaviors of the previous C-type models [19], taking into account the effects of variable supply pressure and leakage acting among the control ports connecting the valve to the motor element (i.e. the eventual PSR variation, from a computational point of view, affects both pressure and flow gains, besides the direct action on the pressure limits). As reported in the previous chapter, as a consequence of the leakage feedback loop these models could be suffering from numerical instabilities and other computational problems; for this purpose, as explained hereafter, the authors propose two possible solutions (i.e. the new C3 and C4 models). The first enhancement proposed by the authors in order to overcome the limits evidenced by the previous models is shown in Fig. 14: to this purpose, it is proposed to overcome the problems related to the interaction between the pressure saturation block and the leakage feedback loop (located downstream of this block) by modifying the formulation of the pressure/flow gain ratio GPQ. As already highlighted in [19-20], even if the GPQ value is almost independent of the differential supply pressure (PSR), the effect of leakage on the regulated pressure downstream of the valve (P12) is less significant for large spool displacements (and in particular when |XS| > XSS). This can be explained by remembering that, with high spool displacements, the control ports areas (regulating the actuation flow QJ) are much greater than internal valve orifices (through which the said leakage flows are drained).

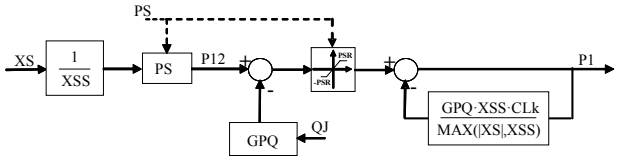

Fig. 14 MODEL C3 block diagram: initial formulation

As reported in [14], under linear conditions the pressure gain GP is almost independent of the spool displacement XS and, therefore, the regulated differential pressure P12 should be calculated as follows:

$$P12 = GP \cdot XS \tag{2}$$

Vice versa, under saturation conditions (i.e. |XS| > XSS), (2) is no longer valid, and the apparent value of conditions the pressure gain GP(PSR,XS) (i.e. related to XS and PSR) decreases progressively as XS increases: therefore, in this case P12 should be calculated as:

$$P12 = GP(PSR,XS) \cdot XS \tag{3}$$

Taking also into account that, in condition of pressure saturation (i.e. |XS| = XSS), P12 is equal to PSR, it is possible to express GP as follows:

$$GP = PSR/XSS \tag{4}$$

To develop a general formulation of GP(PSR,XS) shown in (3) (and defined GPSS in the following), valid both for linear and saturated conditions, (4) should be modified as:

$$GPSS=PSR/\ MAX(|XS|,XSS) \tag{5}$$

where MAX(|XS|,XSS) represents the Matlab function "maximum", which calculates the highest value between | XS | and XSS. Thus, by combining (4) and (5), a new GPSS formulation is obtained depends on the linear GP, the spool displacement XS, and the XSS:

$$GPSS = GP \cdot XSS/MAX(|XS|,XSS) \tag{6}$$

The enhanced pressure gain formulation proposed in (6) is implemented in the leakage feedback loop of MODEL C3 (as shown in Fig. 14) in order to mitigate the shortcomings highlighted in the last section of the previous chapter. For this purpose, the pressure to flow gain ratio GPQ (i.e. GP/GQ) adopted in previous models was modified according to (6): the overall gain of the leakage feedback loop (formerly equal to CLk·GPQ = CLk·GP/GQ) is then modified substituting the constant pressure gain GP (independent to XS) with the proposed GPSS, so obtaining:

$$CLk \cdot GPSS/GQ = CLk \cdot GPQ \cdot XSS/MAX(|XS|,XSS) \tag{7}$$

Also in this case, as has already been done for the first two C-type models, it is possible to pre-resolve the leakage feedback loop obtaining the final formulation shown in Fig. 15 as MODEL C3. A further possible development of the above mentioned C-type models [19], including leakage and variable PSR computational algorithms, is here introduced by the authors as MODEL C4 (shown in Fig. 16).

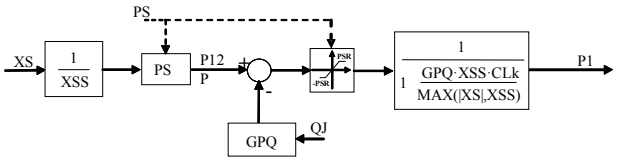

Fig. 15 MODEL C3 block diagram: final formulation

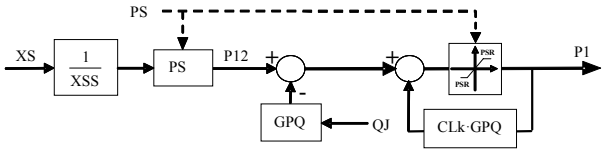

Fig. 16 MODEL C4 block diagram: initial formulation

In this model, in order to employ the invariant GPQ block, the flow feedback sum block has been displaced downstream the GP one, nevertheless being upstream the saturation block PSR. To compute the effects of the variable value of PSR, the model must be compliant not only with variable values of PSR along the simulation run, but also with the related variable values of pressure and flow gains, according to the above discussed assumption of proportionality between GP, GQ and PSR. Theoretically, given that MODEL C4 considers the leakage loop including the pressure saturation block (limited within the values ±PSR), the authors expect this formulation results as more realistic than MODELS C1, C2, C3. It should be noted that this computational layout is not necessarily consistent with the previous analytical solution of the loop itself (as proposed for instance in Fig. 15), that is able to prevent computational instabilities, and so, MODEL C4 could generate transitory numerical troubles. Consequently, as regards this model, a different solution of the problem is considered: to preventing any instantaneous dynamics, the leakage loop is converted in a first-order subsystem characterized, for example, by a hydraulic capacity. By giving a proper value to the related hydraulic time constant τ (consistent with the integration step DT adopted in the numerical simulation code), these computational instabilities can be avoided, but the dynamic behavior of the whole system may be improperly modified. At the beginning of each new calculation step of the numerical algorithm simulating the MODEL C4 response, a brief simulation of the dynamics of the leakage loop is iteratively run, until the reasonable stabilization of its pressure and flow values. This iterative method is based on the first-order pseudo-dynamic approach proposed by Borello et al. in [21-22]. As a consequence, the final evolution of this model, similarly developed as the previous MODEL A, is reported in Fig. 17: in this figure, the "short run" of the leakage dynamics is dash-outlined with gray background. Merits or demerits of these models, characterized by a semi-empirical formulation, are related to their ability to properly describe the behavior of the valve, represented by the diagrams reporting their "characteristics" and by the simulations of a typical servomechanism employing it.

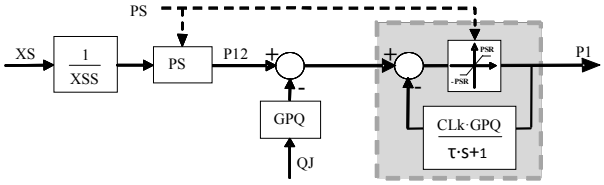

Fig. 17 MODEL C4 block diagram: final formulation

The related considerations are presented in the following paragraph. To this purpose, some dedicated computational programs have been prepared.

V. Fluid-Dynamic Characteristics P12 - XS

On the basis of each mathematical model considered and the related algorithm, a numerical simulation program calculating the fluid-dynamic characteristics of the selected valve has been conceived. The results provided by this program consist of diagrams in which the differential pressure P12 acting on the motor element is calculated, for each value of PSR and CLk, as a function of the displacement of the valve spool XS, having the flow QJ through the piston as a parameter. The following results have been obtained for a valve characterized by XSS = 0.1 mm and GPQ = $6.667 \cdot 10^{11}$ Pa·s/m^3, independent on PSR, relating the values of GP or GQ and PSR each other.

Taking into account the previous work (reported as [19]), in this paper authors compare the most elementary models (i.e. A and B models) with C-type models, evaluating their merits and defects and comparing them with the reference high-fidelity model HD (its fluid-dynamic characteristic is shown in Fig. 3).

In Fig. 18 (MODEL A) the results concern the values of CLk=0 m^3/s/Pa, GQ=0.3 m^2/s, PSR=20 MPa, GP=$2 \cdot 10^{11}$ Pa/m. The slope of the zero-flow curve is equal to the value of GP, because of the effect of CLk=0, as it appears correct, while no saturation is present, according to the model structure. Higher values of QJ refer to lower P12 ones, like expected, not only in the present case but also in the following, as a consequence of the sign assumptions.

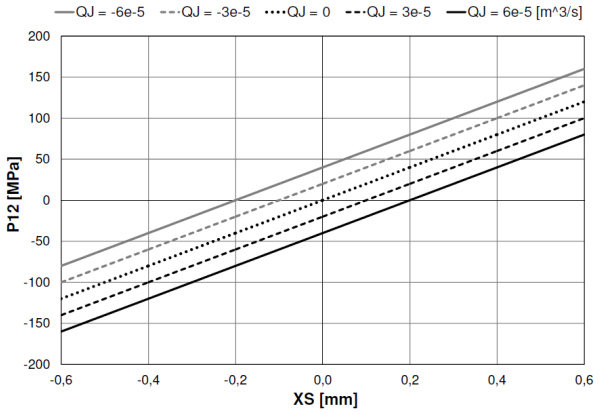

Fig. 18 MODEL A in case of CLk = 0 m^3/s/Pa and PSR = 20 MPa

Figure 19 shows the characteristic P12–XS concerning the same values as before except for CLk = $2 \cdot 10^{-13}$ m^3/s/Pa.

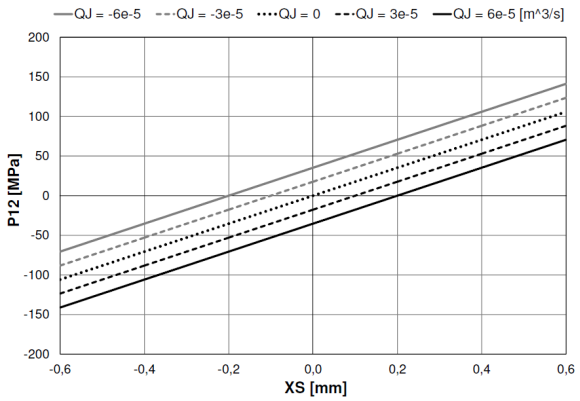

Fig. 19 MODEL A – CLk = $2 \cdot 10^{-13}$ $m^3/s/Pa$ and PSR = 20 MPa

The slope of the zero-flow curve is constant and lower than the value of GP, because of the effect of CLk > 0 (see Fig. 19).

Figure 20 shows the results related to the same values of Fig. 16 except for PSR = 12 MPa. The zero-flow slope is reduced because of the effects of both CLk > 0 and low PSR.

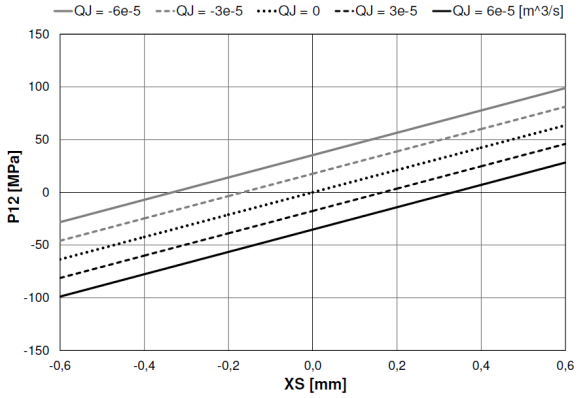

Fig. 20 MODEL A – CLk = $2 \cdot 10^{-13}$ $m^3/s/Pa$ and PSR = 12 MPa

Figure 21 reports the results of MODEL B obtained with CLk = $2 \cdot 10^{-13}$ $m^3/s/Pa$, GQ = 0.3 m^2/s, PSR = 20 MPa, GP=$2 \cdot 10^{11}$ Pa/m. Also in this case the slope of the zero-flow curve, in its central portion (linear conditions), is lower than the value of GP, because of the effect of CLk > 0.

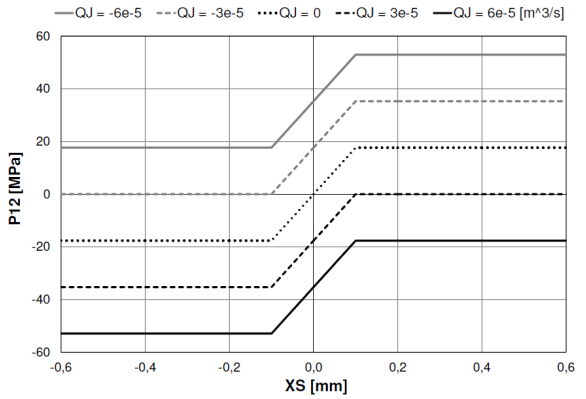

Fig. 21 MODEL B – CLk = $2 \cdot 10^{-13}$ $m^3/s/Pa$ and PSR = 12 MPa

In Fig. 22 (MODEL C1) is shown the fluid-dynamic characteristic concern the values of CLk = 0 $m^3/s/Pa$, GQ = 0.3 m^2/s, PSR = 20 MPa and GP =$2 \cdot 10^{11}$ Pa/m. The slope of the zero-flow curve in its central portion, is equal to the value of GP, because of the effect of CLk = 0.

Under saturation conditions, the PSR is calculated as invariant with respect to XS for all QJ values, as a consequence of the model structure. It represents the inability of the model to correctly calculate the high values reached by the differential pressure P12 in case of "water hammer", related to a sudden centering of the valve spool when the drive element is still rapidly moving.

It should be noted that under linear conditions, with the same spool displacement XS, the highest values of differential pressure P12 are obtained for strongly negative QJ flows (and vice versa). This behavior can be explained by referring to the adopted sign convention (Fig. 12). These considerations do not apply only to the present case, but also to the following ones.

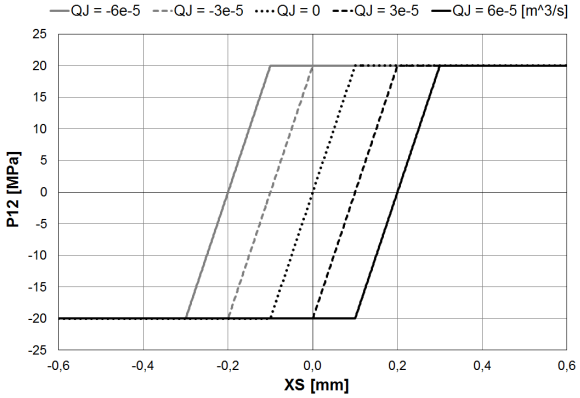

Fig. 22 MODEL C1 – CLk = 0 $m^3/s/Pa$ and PSR = 20 MPa

In Fig. 23 (MODEL C1) the results concern the same values as before, except for CLk = $2\ 10^{-13}$ $m^3/s/Pa$. The slope of the zero-flow curve, in its central portion, is lower than the GP value, due to the effect of CLk > 0, and the saturation value of P12, represented by PSR, cannot be achieved, because the block that calculates the effect of leakage is placed downstream of saturation, as shown in Fig. 12.

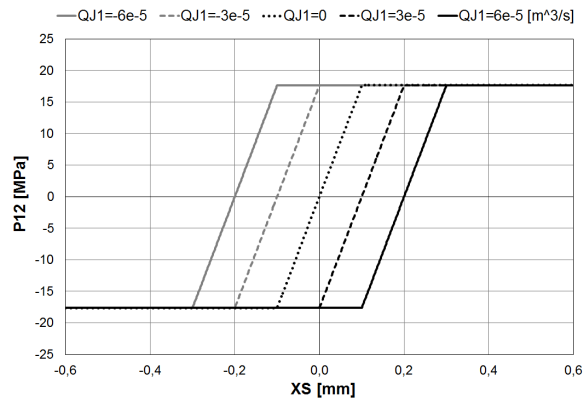

Fig. 23 MODEL C1 – CLk = $2 \cdot 10^{-13}$ $m^3/s/Pa$ and PSR = 20 MPa

Figure 24 shows the results related to the same case of Fig. 22 except for PSR = 12 MPa. The slope of the zero-flow curve is further reduced due to the effects of both CLk > 0 and reduced differential supply pressure PSR. As in Fig. 19, the algorithm shows the inability of P12 to reach the PSR value in saturation condition; it can be considered a defect under certain conditions, but it has been partially solved by the new models proposed by the authors

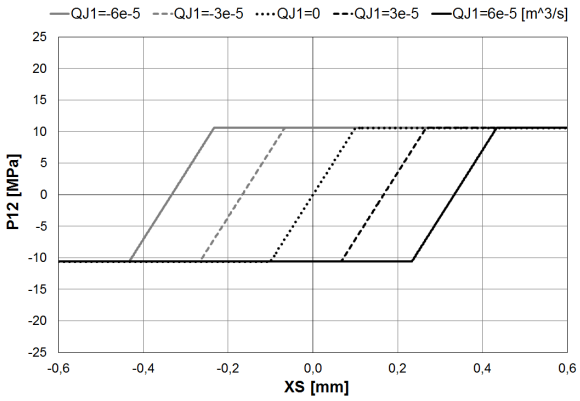

Fig. 24 MODEL C1 – CLk = $2 \cdot 10^{-13}$ $m^3/s/Pa$ and PSR = 12 MPa

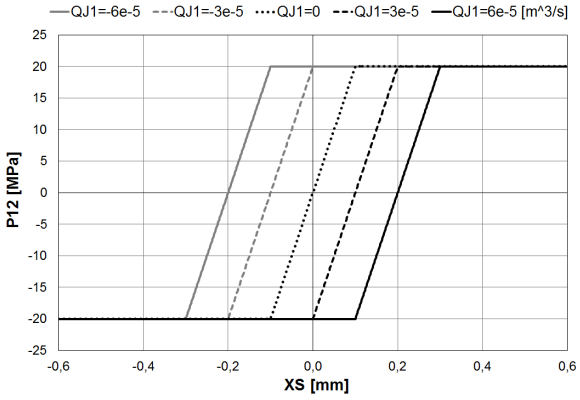

Fig. 25 MODEL C2 – CLk = 0 $m^3/s/Pa$ and PSR = 20 MPa

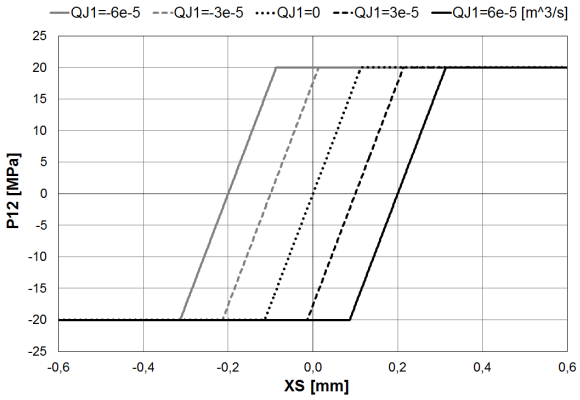

Fig. 26 MODEL C2 – CLk = $2 \cdot 10^{-13}$ $m^3/s/Pa$ and PSR = 20 MPa

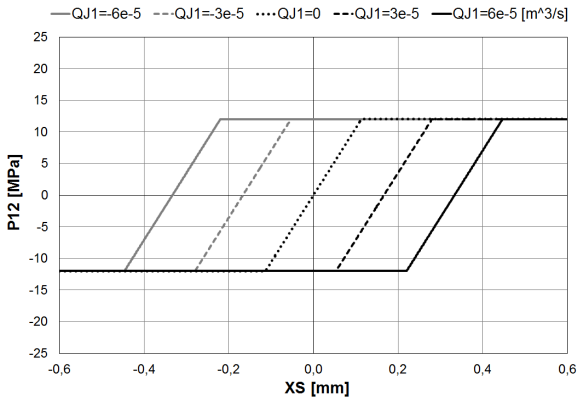

Fig. 27 MODEL C2 – CLk = $2 \cdot 10^{-13}$ $m^3/s/Pa$ and PSR = 12 MPa

In Fig. 25 (MODEL C2) is shown the fluid-dynamic characteristic regarding the values of CLk = 0 $m^3/s/Pa$, GQ = 0.3 m^2/s, PSR = 20 MPa and GP = $2 \cdot 10^{11}$ Pa/m. As can be expected, it is identical to Fig. 22, because the different architecture of the algorithm has no effect when the CLk is null; so, the same considerations, as in Fig. 18, can be done.

In Fig. 26 (MODEL C2) the results concern the same values as before, except for CLk=2 10^{-13} $m^3/s/Pa$. The slope of the zero-flow curve, in its central portion (linear conditions), is lower than the value of nominal GP, because of the effect of CLk > 0, but the saturation value of P12, represented by PSR, is correctly reached because the saturation block is positioned downstream of the leakage loop, as shown in Fig. 13.

Figure 27 (MODEL C2) shows the results related to the same values of Fig. 26 except for PSR = 12 MPa. The slope of the zero-flow curve is further reduced because of the effects of both CLk > 0 and low PSR. As in Fig. 26 the saturation value of P12 can be correctly reached.

In Fig. 28 (MODEL C3) is shown the fluid-dynamic characteristic regarding the values of CLk = 0 $m^3/s/Pa$, GQ = 0.3 m^2/s, PSR = 20 MPa and GP = $2 \cdot 10^{11}$ Pa/m. As can be expected, also in this case the same considerations already applied for the cases of Figs. 18-21: also the fluid-dynamic characteristic is the same since the different architecture of the algorithm has no effect when the CLk is null.

In Fig. 29 the results concern the same values previously considered, with the exception of the leakage coefficient CLk = 2 10^{-13} $m^3/s/Pa$. The structure of the MODEL C3 is conceived to overcome the shortcomings of the previous models: to this purpose, the general layout of the block diagram is similar to the MODEL C1, but the leakage block employs a value of GPQ affected by the saturation correction, as reported in Fig. 15 (block diagram). The slope of the zero-flow curve, in its central portion, is lower than the value of GP, because of the value of CLk > 0, but the attempt to take correctly into account the effect of the saturation of P12 is not successful, because, in case of low values of spool displacement XS, the algorithm introduces further inaccuracies, as the Fig. 29 shows. In fact, usually the values of P12 related to QJ ≠ 0 and small XS are greater or certainly not lower than the saturation value PSR.

Figure 30 (MODEL C3) shows the results related to the same values of Fig. 29 except for PSR = 12 MPa. The slope of the zero-flow curve is further reduced because of the effects of both CLk >0 and low PSR. As in Fig. 29 the saturation conditions of P12 cannot be correctly computed.

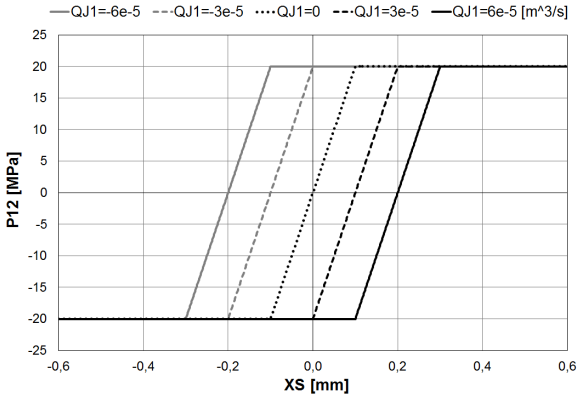

Fig. 28 MODEL C3 – CLk = 0 m^3/s/Pa and PSR = 20 MPa

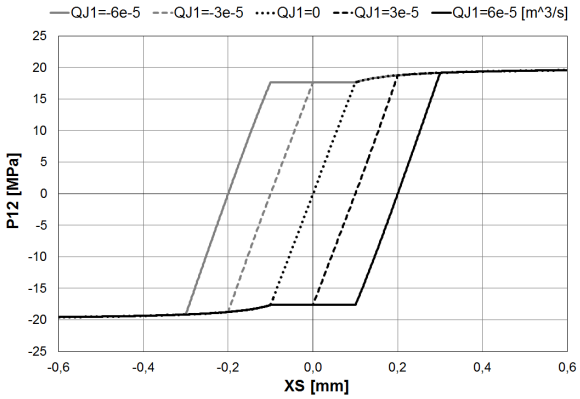

Fig. 29 MODEL C3 – CLk = $2 \cdot 10^{-13}$ m^3/s/Pa and PSR = 20 MPa

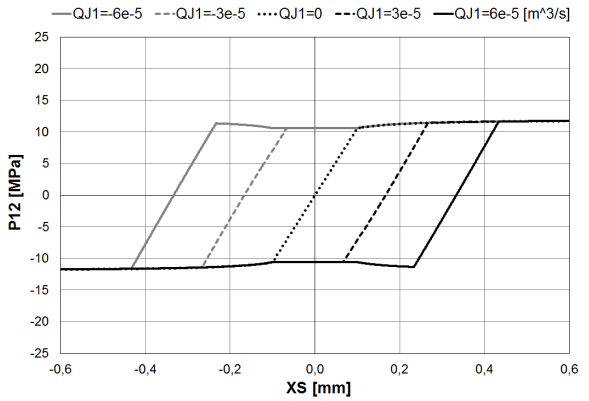

Fig. 30 MODEL C3 – CLk = $2 \cdot 10^{-13}$ m^3/s/Pa and PSR = 12 MPa

In Fig. 31 (MODEL C4) is shown the fluid-dynamic characteristic regarding the values of CLk = 0 m^3/s/Pa, GQ = 0.3 m^2/s, PSR = 20 MPa and GP =$2 \cdot 10^{11}$ Pa/m.

As can be expected, it is identical to Figs. 22, 25 and 28, because the different architecture of the algorithm has no effect when the CLk is null; the same considerations already reported for previous models are valid also in this case.

In Fig. 32 (MODEL C4) the results concern the same values as before, except for CLk=2 10^{-13} m3/s/Pa. Also for this model, the slope of the zero-flow curve, in its central portion (linear conditions), is lower than the nominal GP value, due to the effect of CLk > 0; the saturation value of P12 is calculated correctly because the pressure saturation block, located inside the action branch of the leakage ring (as shown in the block diagram of Fig. 13), still reaches its limit values ±PSR.

Figure 33 shows the results related to the same values of Fig. 32 except for PSR = 12 MPa. The slope of the zero-flow curve is further reduced because of the effects of both CLk > 0 and low PSR; as in Fig. 32 the saturation value of P12 can be correctly reached. As regards Figs. 31-33, it must be noted that, contrary to all expectations, the MODEL C4 is not able to give any improvement with respect to MODEL C2, in spite of its higher complexity; the fact that MODEL C4, despite the much more complex architecture of calculating the effects due to saturation and leakage, produces the same results as MODEL C2 is attributable to the inability of the saturation block to produce an upstream action through the feedback loop, since the pressure limits themselves exclude any effect.

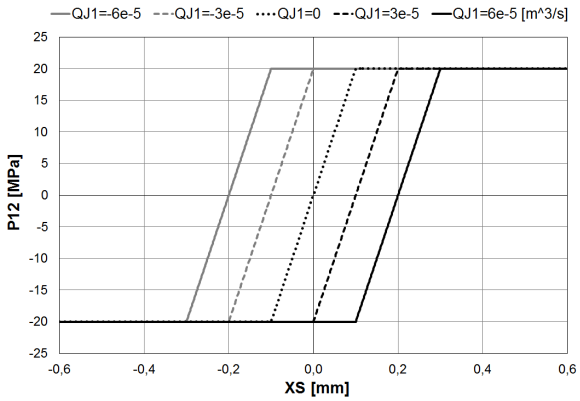

Fig. 31 MODEL C4 – CLk = 0 m^3/s/Pa and PSR = 20 MPa

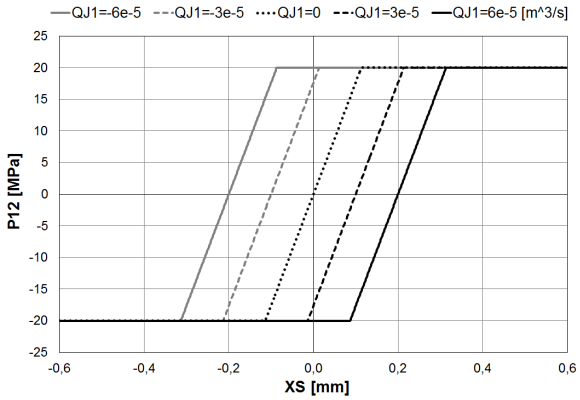

Fig. 32 MODEL C4 – CLk = $2 \cdot 10^{-13}$ m^3/s/Pa and PSR = 20 MPa

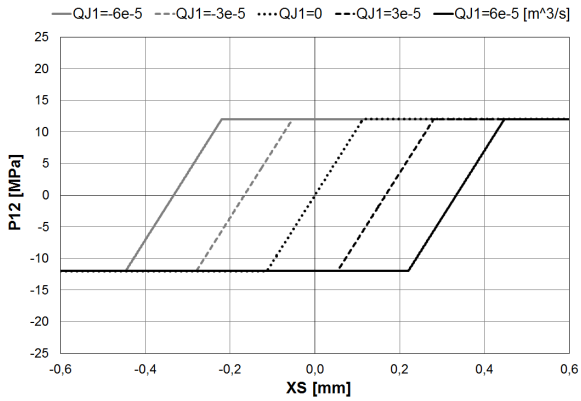

Fig. 33 MODEL C3 – CLk = $2 \cdot 10^{-13}$ $m^3/s/Pa$ and PSR = 12 MPa

VI. Numerical Results Of EHA Test-bench

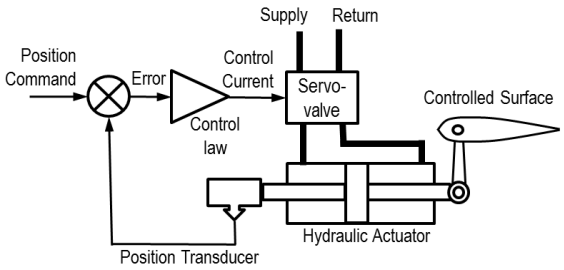

Fig. 34 schematic of the electrohydraulic actuator (EHA) [23]

In order to compare the behavior of the different models and related computational algorithms concerning the fluid-dynamics of the control valve equipping a hydraulic actuation servomechanism, a typical onboard system was considered.

The conceptual schematic of this electrohydraulic actuator (EHA) system is shown in Fig. 34. It mainly consists of a Power Control and Drive Unit (PCDU) and its control is performed by an Electronic Control Unit (ECU), not shown in Fig. 34, closing the position control loop. The PCDU contains hydraulic piston, and control electro-hydraulic two stage servo-valve. The EHA model takes into account the electrical, hydraulic and mechanical characteristics of all the system components which are relevant to the purpose.

In particular, the model is able to compute the following:

1) inertia, viscous and eventual Coulomb friction regarding the hydraulic piston;
2) third order electromechanical dynamic model of the servo-valve with first and second stage ends of travel and simplified fluid-dynamic model, containing the motor element internal leakage.

The simulations shown in this chapter in Figs. 35 to 40 represent the dynamic response of the aforementioned EHA to a combination of position controls (Com), external loads (FR) and variations in the hydraulic supply pressure (PSR): this sequence of input has been appropriately defined to highlight the performance of the proposed fluid dynamic-models and their effect on the dynamic behavior of the EHA simulation test-bench.

As will be shown in the following of this section, by comparison of Figs. 35-40 it is possible to highlight the main differences, strengths and weaknesses of the simulation models obtained by implementing the fluid-dynamic model of the SV coil using the different algorithms proposed in the previous chapters: MODEL A (Fig 35), MODEL B (Fig 36), MODEL C1 (Fig 37), MODEL C2 (Fig. 38), MODEL C3 (Fig. 39) and MODEL C4 (Fig. 40). These simulations will be compared with Fig. 41, representing the dynamic response of the same numerical simulation model of the servomechanism equipped with a high-fidelity valve fluid dynamics simulation model (called HD MODEL); as shown in [14], it can be considered a reliable tool capable of performing accurate simulations of the SV behaviors and, therefore, it is adopted in this section as a reference for evaluating the said simplified models.

According to [19], the time history applied to Com consists of a series of three step commands ranging from 0 m (initial position) to 0.02 m at Time =0 s, to 0.03 m at 0.3 s, to 0.02 m at 0.75 s. The time history of the load FR acting on the motor element, having null value since 0 s to 0.2 s, reaches the final constant value (10400 N) through a step change at Time = 0.2 s; so, the actuation run of the system following the first step command is unloaded, while FR acts as an opposing or aiding load during the second run (starting at Time = 0.3 s) or the third one (Time = 0.75 s and following) respectively.

The time history of the supply/return differential pressure PSR consists of three time intervals, each characterized by a constant differential pressure value: during the first and the third time interval (Time since 0 s to 0.35 s and since 0.45 s to the end of simulation, respectively), the 20 MPa nominal value is kept as a constant (corresponding stall load FR = 14.1 kN), while during the second (0.35 to 0.45 s) time interval the constant 12 MPa reduced value (related stall load FR = 8.5 kN) is performed through two-step changes. So, the effect of a temporary supply pressure drop, acting during the opposing load actuation run, is evaluated. All these simulations have been run with a leakage coefficient CLk=$2 \cdot 10^{-13}$ $m^3/s/Pa$.

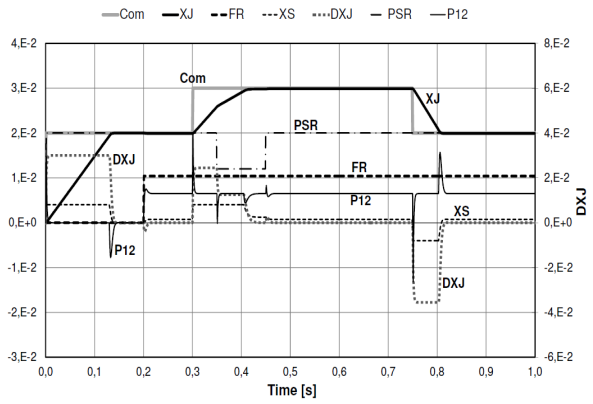

Fig. 35 EHA dynamic response – MODEL A

Figure 35 shows the dynamic behavior of the system according to MODEL A, which can be compared with the high definition model of Fig. 41.

The simulation of the unloaded actuation run is sufficiently accurate, notwithstanding higher starting accelerations and lower stopping decelerations, as shown by the differential pressure P12 acting on the motor. Similar considerations can be done in case of aiding load run, while the opposing load actuation travel shows a markedly different behavior: according to MODEL A, the effect of the opposing load on the actuation rate is underestimated and, when the supply pressure drops, the system back movement is completely absent, as a consequence of the typical MODEL A inability to compute the correct P12 saturation value. In loaded and motionless conditions the spool displacement is correctly not null, according to the corresponding GP value.

Figure 36 shows the dynamic behavior of the system that implements MODEL B. Comparing it with the HD MODEL it is possible to highlight the typical shortcomings that afflict it: in particular, MODEL B underestimates actuation rate in large spool displacement conditions, due to the overestimation of the relative damping action: in fact, when XS > XSS, the MODEL B computes the same flow as XS = XSS, so acting as XSM = XSS. However, the evaluation of FR and PSR effects on the underestimated actuation rate seems to be more reasonable than in MODEL A; as a consequence, any other consideration is out of place and unnecessary.

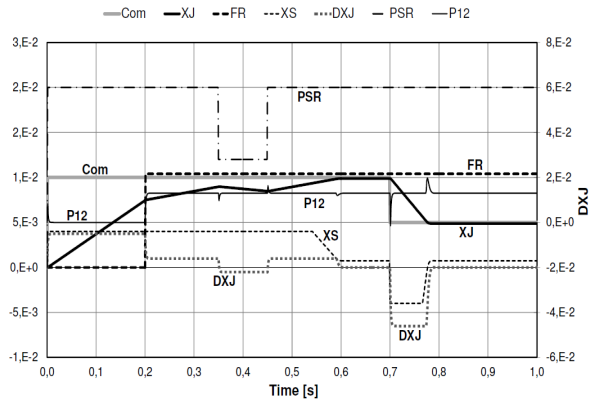

Fig. 36 EHA dynamic response – MODEL B

Figures 37, 38 and 39 show the dynamic responses of the EHA numerical model implementing MODEL C1, MODEL C2, MODEL C3 respectively; also these dynamics will be compared with the corresponding response of the system equipped with high-fidelity SV model (i.e. HD MODEL).

Both the unloaded and the aiding load actuation runs are rather accurately simulated, in spite of lower stopping deceleration and slightly higher starting accelerations, as the P12 behavior proves. The opposing load actuation runs reveal some significant discrepancies with respect to HD MODEL: the load effect on the system actuation rate, in terms of reduction of the rate itself, is underestimated and, when the supply pressure drops, the system back movement is overestimated, performing an incorrect constant back acceleration.

Further, the acceleration following a spool displacement change keeps a constant value along a relevant part of the acceleration transient, rather than the much more plausible asymptotic trend reported in HD MODEL, similar to a first order response which follows a step input; the reason lies in the too much simplified (and partially unsatisfying) action of the differential pressure P12 saturation block implemented in the algorithms shown by the block diagrams represented in Figs. 12, 13 and 15.

In these conditions, the results given by MODEL C1, MODEL C2 and MODEL C3 are unreliable with respect to the surely more accurate HD MODEL ones (shown in Fig. 41), but the computational inaccuracies ascribable to MODEL C2, MODEL C3, MODEL C1 are high, higher and much higher respectively and are emphasized by increasing Clk values in MODEL C3 and C1. Similar considerations can be made regarding the stop following the run in aiding conditions, calculating an incorrectly delayed action.

The aforesaid observations prove the substantial inability of these model (i.e. MODEL C1, C2, and C3) to take correctly into account the damping action related to the flow crossing the valve passageways when load and deceleration require particularly high values of differential pressure P12, eventually exceeding PSR (e.g. in water hammer condition).

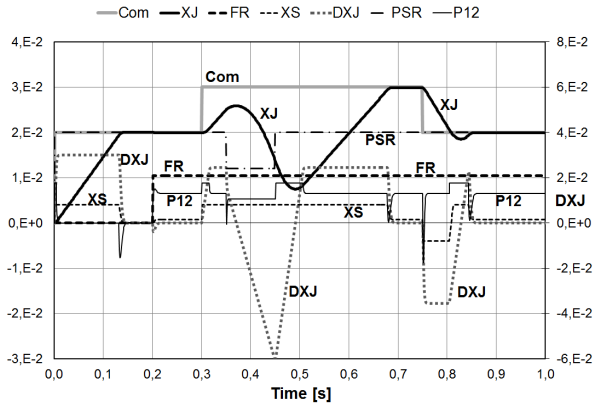

Fig. 37 EHA dynamic response – MODEL C1

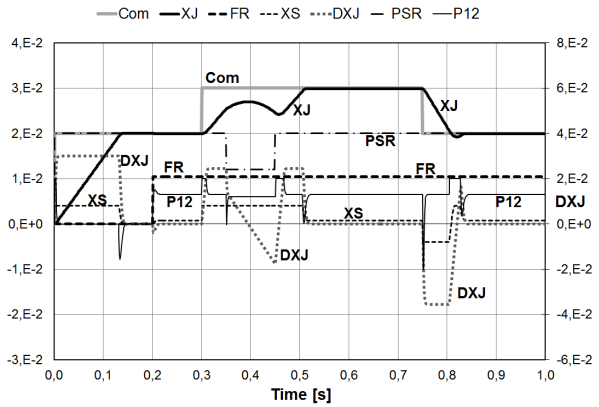

Fig. 38 EHA dynamic response – MODEL C2

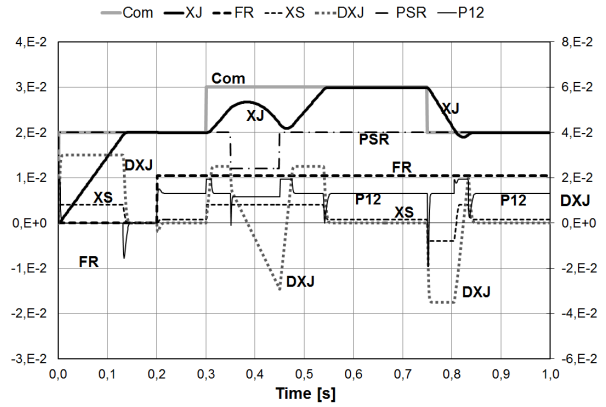

Fig. 39 EHA dynamic response – MODEL C3

This improper behavior depends on the restrictions imposed on the simulated P12 pressure level, without regarding the specific working conditions of the system; in fact, MODEL C2 limits the P12 amount within ± PSR, whatever CLk value is, MODEL C3 and mainly MODEL C1 limit P12 within ± PSR*, where PSR* decreases more and more (compared to the nominal value of PSR), as the value of CLk increases (i.e. PSR* is to be intended as PSR reduced by leakage effect).

In case of an actual system having the valve spool fully displaced (i.e. XS = XSM), the stall load characterizing the piston decreases as CLk grows; this behavior, correctly simulated both in MODEL C1 and in MODEL C3, makes them more accurate than MODEL C2 but, in the other hand, it must be noted that when an over-stall load is reached the inability to calculate properly high P12 values represents a severe shortcoming, mainly for MODEL C1 and MODEL C3.

Instead, regarding MODEL C4 (shown Fig. 40), it must be noted that, contrary to all authors expectations, also in this case it is not able to give any significant improvement with respect to the simpler MODEL C2 [19]. Despite its greater complexity and possible numerical stability problems associated with the first-order model of leakage ring, MODEL C4 gives the same results of MODEL C2; these behaviors are due to the substantial inability of the saturation block to generate any influence upstream, through the leakage feedback loop, because the pressure limits themselves cut off any effect.

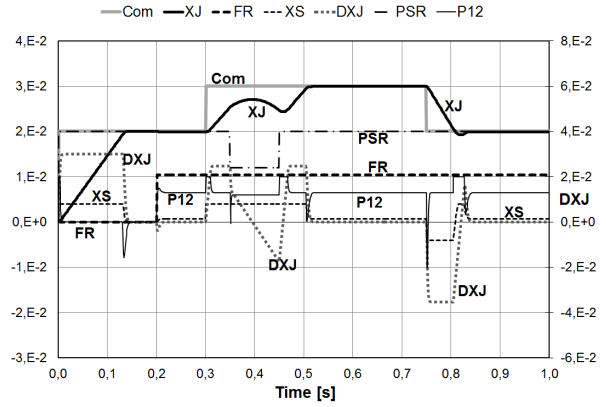

Fig. 40 EHA dynamic response – MODEL C4

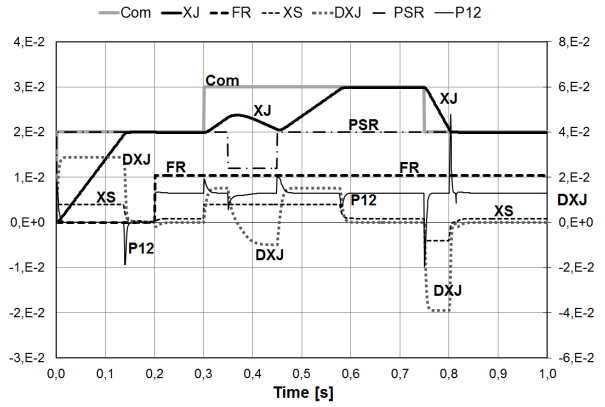

Fig. 41 EHA dynamic response – HD MODEL

VII. Conclusion and Future Perspectives

The analysis of the performances of the seven different fluid dynamic models of valve considered in this document (A, B C1, C2, C3, C4 and HD models) clearly highlights the few advantages and the shortcomings of the simplified models proposed so far by the authors. The evaluation of transients (accelerations, decelerations) is more or less deficient (over- or under-estimated) in all the models. The first model considered (MODEL A), which shows a marked insensitivity to the action of the external load FR, clearly shows all its limitations (that are due to its extremely simplified linear formulation).

MODEL B is even less accurate than MODEL A and, in particular, it is completely unsatisfactory when XS> XSS, while it is quite equivalent to MODEL A if XS ≤ XSS.

As regards the C-type models, it must be noted that the simulations of both the unloaded and aiding loaded actuation runs are sufficiently accurate in MODEL C1, C2, C3 and C4. The computational evaluations of the actuation run in conditions of opposing load are generally unsatisfying, but particularly for MODEL C1 and MODEL C3, because of the overestimation of the actuation rate itself. The over-stall condition, when an actuation run is commanded in opposing load condition, produces a substantial overestimation of the actuation speed DXJ in all the proposed models (in comparison with the HD MODEL) but it is much more marked in the case of MODEL C3 and especially MODEL C1.

In general, the proposed C-type models are not completely capable of overcoming the shortcomings of previous models.

However, especially under saturation conditions, MODEL C2 appears to be sufficiently more accurate than others, particularly in the case of low QJ value, providing some small improvement with respect to all the other models here considered. Instead, as already mentioned, it should be noted that, contrary to all expectations, MODEL C4 is not able to make any substantial improvement compared to C2, despite the greater complexity, the higher computational cost and the possible problems of numerical convergence. In conclusion, the proposed approaches to the modeling of typical non-linear fluid dynamics, which characterize the proportional control valves, present some gaps, in particular in non-linear fields.

The proposed new models, while trying to propose more efficient solutions, have not proved to be decisive. In the authors' opinion, further studies are needed, capable of producing more efficient algorithms, to improve the ability to perform acceptable simulations of all possible working conditions.

TABLE I. LIST OF SYMBOLS

Symbol	Definition	Units (SI)
CLk	Valve leakage coefficient	$m^3/(Pa \cdot s)$
Com	Servomechanism position command	m
DXJ	Motor element velocity	m/s
FR	Load acting on the motor element	N
GP	Valve pressure gain	Pa/m
GQ	Valve flow gain	m^2/s
GPQ	Pressure to flow gain ratio (GP/GQ)	$Pa \cdot s/m^3$
P12	Actual differential pressure	Pa
P12P	Zero-flow differential pressure	Pa
PSR	Supply/return differential pressure	Pa
QLk	Leakage flow	m^3/s
QJ	Working flow	m^3/s
XJ	Motor element position	m
XSM	Spool end of travel displacement	m
XSS	P12P saturation spool displacement	m

ACKNOWLEDGMENT

The authors wish to extend a heartfelt thanks to Prof. Lorenzo Borello for his valuable teachings and for his support in the conception and development of this research.

REFERENCES

[1] H. E. Merritt, Hydraulic control systems. New York: Wiley, 1967.

[2] T. J. Viersma, Analysis, synthesis and design of hydraulic servo-systems and pipelines. Amsterdam: Elsevier, 1980.

[3] G. Jacazio, L. Borello, "A non-linear model of an electro-hydraulic servo system with axial piston hydraulic motor," 7th Interntional Fluid Power Symposium, Bath (UK), 16-18 September 1986.

[4] G. Jacazio, L. Borello, "Mathematical Models of Electrohydraulic Servovalves for Fly-by-Wire Flight Control Systems," Mathematical Computational Modelling, vol. 11: Pergamon, 1988, pp. 563–569.

[5] L. Borello, M. D. L. Dalla Vedova, G. Jacazio, M. Sorli, "A Prognostic Model for Electrohydraulic Servovalves," Annual Conference of the Prognostics and Health Management Society, 2009.

[6] E. Urata, "Study of magnetic circuits for servovalve torque motors," Bath workshop on power transmission and motion control, Bath, UK, pp. 269–282, 2000.

[7] E. Urata, "Study on Leakage Flux from Servovalve Torque Motors," The Seventh Scandinavian Intl. Conf. on Fluid Power, Linköping, Sweden, vol. 1, pp. 51–66, 2001.

[8] E. Urata, "Influence of fringing on servovalve torque-motor characteristic," Proc. Fifth JFPS Intl. Symp. on Fluid Power, Nara, vol. 3, pp.769–774, 2002.

[9] E. Urata, "Static Stability of Toque Motors, The Eighth Scandinavian Intl. Conf. on Fluid Power, Tampere, Finland, pp.871–885, 2003.

[10] E. Urata, "Influence of eddy current on torque-motor dynamics," 4th IFK Workshop, Dresden, Germany, pp. 71–82, March 2004.

[11] E. Urata, "One degree of freedom model for torque motor dynamics," International Journal of Fluid Power, vol. 5, no. 2, pp. 35–42, 2004.

[12] E. Urata, "Influence of asymmetry of air-gap in servovalve torque motor," The Ninth Scandinavian Intl. Conf. on Fluid Power, Linkoping, Sweden, 2005.

[13] G. Di Rito, "Experiments and CFD Simulations for the Characterisation of the Orifice Flow in a Four-Way Servovalve," International Journal of Fluid Power, vol. 8, no. 2, FPNI/TuTech, 2007.

[14] M. D. L. Dalla Vedova, "Design of physical-mathematical models suitable for advanced simulation and design of flight control and study related innovative architecture," PhD dissertation (in italian), Politecnico di Torino, 2007.

[15] W. Jia, C. Yin, "CFD Simulation with Fluent and Experimental Study on the Characteristics of Spool Valve Orifice," 2nd International Conference on Computer Engineering and Technology - IEEE, Chengdu, China, 2010.

[16] X. Pan, G. Wang, Z. Lu, "Flow field simulation and a flow model of servo-valve spool valve orifice," Energy Conversion and Management, n.52, pp.3249–3256, Elsevier, 2011.

[17] L. Pace, M. Ferro, F. Fraternale, A. Caimano, P. Maggiore, M. D. L. Dalla Vedova, "Comparative analysis of a hydraulic servo-valve," International Journal of Fluid Power, vol. 14, pp. 53–62, 2013.

[18] P. Dransfield, Hydraulic control systems - design and analysis of their dynamics. Berlin: Springer-Verlag, 1981.

[19] P. Alimhillaj, L. Borello, M. D. L. Dalla Vedova, "Proposal of Innovative Fluid Dynamic Nonlinear Servovalve Synthetic Models," International Journal of Mechanics and Control, vol. 14, no. 2, pp. 39–49, December 2013.

[20] L. Borello, G. Villero, "Comparison between control valves simplified models," XI Congresso Nazionale A.I.D.A.A., Forlì, 14-18 Ottobre 1991.

[21] L. Borello, M. D. L. Dalla Vedova, "Pseudo-dynamic simulation method solving hydraulic stationary problems," International Journal of Mechanics and Control (JoMaC), vol. 8, no. 2, pp. 43–52, 2007.

[22] L. Borello, M. D. L. Dalla Vedova, "A pseudo-dynamic approach to a simple example of structural static problem," XX AIDAA National Congress, Milan, Italy, 2009.

[23] M.D.L. Dalla Vedova, P. Maggiore, L. Pace, "Proposal of Prognostic Parametric Method Applied to an Electrohydraulic Servomechanism Affected by Multiple Failures," WSEAS Trans. on Environment and Development, vol. 10, pp. 478–490, 2014.

Matteo D. L. Dalla Vedova received the M.Sc. and the Ph.D. from the Politecnico di Torino in 2003 and 2007, respectively. He is currently Assistant Professor in the Department of Mechanics and Aerospace Engineering. His research activity is mainly focused on the aeronautical systems engineering and, in particular, is dedicated to design, analysis and numerical simulation of on board systems, study of secondary flight control systems and conception of related monitoring strategies, development of prognostic algorithms for aerospace servomechanism and study of innovative primary flight control architectures.